

Conf-740443--1

DEFORMATION AND FAILURE OF
FAST REACTOR CLADDING DURING
SIMULATED LOSS-OF-FLOW TYPE
TRANSIENTS

By

C. W. Hunter and R. L. Fish

ABSTRACT

The deformation and failure behavior of 20% cold worked Type 316 stainless steel fuel cladding was experimentally determined under thermal transients and internal gas pressures, which simulated hypothetical loss-of-flow accident conditions. Both unirradiated and EBR-II irradiated tubular cladding specimens ($7.4-9.0 \times 10^{21}$ n/cm², $E_n > 0.1$ MeV) were subjected to heating rates of 10 and 200°F/sec, with hoop stress loadings of 1300 to 6480 psi. These test conditions produced cladding failure at temperatures from 2000 to 2400°F.

In unirradiated cladding the failure temperature increased and the strains at failure decreased with decreasing hoop stress levels. Similar trends were observed in the EBR-II irradiated cladding, except that the failure ductilities were greatly reduced and the failure temperatures were moderately reduced.

The results demonstrate that the ductility of cladding will not be so great as to permit excessive cladding deformations which could interfere with coolant flow. Beginning-of-life pin gas pressures are insufficient to produce failures except at very high temperatures (2400°F), where the failure strains are only about 0.5% in unirradiated cladding. For irradiated cladding, even after only low levels of irradiation, the ductility is sufficiently reduced for all conditions that coolant flow could not be impaired.

Hanford Engineering Development Laboratory

Operated by the
**Westinghouse
Hanford Company**

A Subsidiary of
Westinghouse Electric
Corporation

for the United States
Atomic Energy Commission
Contract No. AT(45-1)-2170

MASTER

NOTICE

This report was prepared as an account of work sponsored by the United States Government. Neither the United States nor the United States Atomic Energy Commission, nor any of their employees, nor any of their contractors, subcontractors, or their employees, makes any warranty, express or implied, or assumes any legal liability or responsibility for the accuracy, completeness or usefulness of any information, apparatus, product or process disclosed, or represents that its use would not infringe privately owned rights.

DISTRIBUTION OF THIS DOCUMENT IS UNLIMITED *See*

DISCLAIMER

This report was prepared as an account of work sponsored by an agency of the United States Government. Neither the United States Government nor any agency thereof, nor any of their employees, makes any warranty, express or implied, or assumes any legal liability or responsibility for the accuracy, completeness, or usefulness of any information, apparatus, product, or process disclosed, or represents that its use would not infringe privately owned rights. Reference herein to any specific commercial product, process, or service by trade name, trademark, manufacturer, or otherwise does not necessarily constitute or imply its endorsement, recommendation, or favoring by the United States Government or any agency thereof. The views and opinions of authors expressed herein do not necessarily state or reflect those of the United States Government or any agency thereof.

DISCLAIMER

Portions of this document may be illegible in electronic image products. Images are produced from the best available original document.

NOTICE

This report was prepared as an account of work sponsored by the United States Government. Neither the United States nor the United States Atomic Energy Commission, nor any of their employees, nor any of their contractors, subcontractors, or their employees, makes any warranty, express or implied, or assumes any legal liability or responsibility for the accuracy, completeness or usefulness of any information, apparatus, product or process disclosed, or represents that its use would not infringe privately owned rights.

Hanford Engineering Development Laboratory

Operated by the

**Westinghouse
Hanford Company**

A Subsidiary of
Westinghouse Electric
Corporation

for the United States
Atomic Energy Commission
Contract No. AT(45-1)-2170

P.O. Box 1970 Richland, Wa. 99352

DEFORMATION AND FAILURE OF FAST REACTOR CLADDING
DURING SIMULATED LOSS-OF-FLOW TYPE TRANSIENTS

By

C. W. Hunter and R. L. Fish

INTRODUCTION

The potential for fuel cladding to extensively balloon, under internal pressures at high temperatures, and to interfere with coolant flow has received considerable attention in recent years.⁽¹⁻⁴⁾ The referenced investigations have dealt with light water reactor Zircaloy fuel cladding; concern over a similar phenomenon in fast reactor 20% cold worked Type 316 stainless steel cladding has been expressed. Results of this present study indicate that coolant blockage by excessive cladding deformation cannot be a problem.

The 20% cold worked Type 316 stainless steel cladding does not exhibit extensive ductility in the normal service temperature range; from 600 to 1400°F the burst ductility of 20% cold worked Type 316 cladding is 1 to 4%.⁽⁵⁾ However, above 1600°F recovery, recrystallization, and annealing of the cold worked condition can occur in short times.⁽⁶⁾ For example, the results of Paxton⁽⁷⁾ revealed that the annealing rate is 100 times faster at 1700°F than at 1600°F and if extrapolated would suggest that annealing occurs in less than a second at 1900°F. Hence, one could be led to believe that the high cladding temperatures achieved during certain hypothetical LOF⁽⁸⁾ accidents may produce in situ annealing. Such annealing would potentially be sufficient to increase ductility to the extent that cladding ballooning could interfere with coolant flow.

During a transient above the steady state fuel cladding irradiation temperature, the strength, ductility and microstructure of cold worked and irradiated cladding are altered. The extent of such alteration during a transient is dependent upon the temperature attained, as well as the heating rate to that temperature. Therefore, in order to precisely define the pertinent mechanical behavior during possible reactor transients, data must be generated under experimental conditions in which the temperature ramps of the transients are duplicated.

The purpose of this work was to experimentally determine the cladding strains caused by internal gas pressures at high cladding temperatures and heating rates typical of those occurring during certain hypothetical LOF accidents. The deformation and failure behavior of both unirradiated and irradiated, pressurized, 20% cold worked Type 316 stainless steel prototypic FTR cladding specimens were studied.

SIMULATED TRANSIENT TESTING

Both unirradiated and irradiated cladding specimens were subjected to simulated reactor thermal transient tests. All irradiated specimens were tested to failure.

A few unirradiated specimens were tested to failure, but more were terminated before failure to define deformation vs. temperature behavior. Two thermal transients of 10°F/sec and 200°F/sec were used. The loading conditions used were internal gas pressures of 180, 450, and 750 psi (hoop stresses of 1300, 3240, and 5400 psi) from an initial or steady-state temperature of 1110°F, and 180, 500, and 900 psi internal temperature of 1350°F.

Cladding Specimens

The specimens used in this study were cut from 20% cold worked Type 316 stainless steel tubing, which was prototypic of FTR fuel pin cladding. The dimensions of this tubing were 0.230 in. O.D. x 0.015 in. wall. Both unirradiated and irradiated specimens were 2.45 in. long.

The specimens were irradiated to fluences of 0.74 and 0.9 x 10²² n/cm² ($E_n > 0.1$ MeV) at temperatures of 1050-1060°F and 1410-1420°F, respectively. The specimens irradiated at the 1050-1060°F temperatures were transient tested from an initial temperature of 1110°F and the 1410-1420°F specimens from an initial temperature of 1350°F.

The EBR-II irradiation was performed in sodium-filled capsules to minimize temperature gradients in the specimens caused by nuclear heating. The size of the gas gaps between the capsules and M-1A irradiation pins were adjusted to obtain the desired irradiation temperatures. The actual irradiation temperatures were determined by postirradiation examination of melting point sentinels and silicon carbide monitors that were placed in the capsules prior to irradiation. The fluence for each specimen level was determined on the basis of the dosimetry test performed during run 31F of the EBR-II. (9)

Test Technique

Swagelok fittings were used to provide specimen end-closure and to attach a high-pressure line to the specimen. The specimens were pressurized with argon gas. The primary pressure measurement was by a calibrated Heise gauge. During the transient test, pressure was monitored by a transducer and strip chart recorder. The pressure did not increase by more than 2% throughout the transient test. The total system volume was 0.7 cu. in., and its availability to the specimen was unrestricted.

Specimen heating was provided by an induction generator and coil. Steady-state temperatures along the gauge length were within ±10°F and temperature variations during a transient were ±10°F for 10°F/sec rates and ±30°F for 200°F/sec rates.

Strain Measurement

The diametral strain information reported here was obtained by taking diameter measurements with a micrometer at ~0.1 inch increments along the axis of the specimen and extracting from the resultant strain profile either the maximum specimen strain in the case of interrupted tests or a diametral strain away from the failure site in the case of specimens tested to failure. Total hoop strain at the failure site was determined by metallographic means, using a rotating traveling micrometer microscope. Values for the radii at various angles around the perimeter at the failure site were used to calculate the total hoop (or circumferential) deformation with the use of a computer code developed specifically for this application. The total hoop strain at the failure site is the maximum strain exhibited

by the cladding and is the appropriate measure with which to evaluate the potential for ballooning to interfere with coolant flow. The diametral strain value away from the failure is believed to be the maximum strain prior to the specimen becoming structurally unstable under constant-pressure gas loading.

RESULTS

Unirradiated Cladding

The measured strain values (diametral and total hoop) and termination or failure temperatures attained during the thermal transients for the unirradiated specimens are presented in Table I along with the pertinent test parameters. Figure 1 illustrates the strain values of both the terminated and failed tests as a function of temperature attained during the transient. For the specimens which failed, the diametral strain away from the failure site and the total hoop strain at the failure site are described by lines that decrease with increasing temperature. The failure strain and failure temperature are dependent on the thermal transient rate and hoop stress level. The diametral strain values from the interrupted tests are also plotted in Figure 1 and were used to define the curves of deformation behavior prior to failure. Four curves of deformation-temperature behavior are shown for two load ranges (5400-6480 psi and 3240-3600 psi hoop) at the two heating rates. The deformation-temperature curves reveal that the rate of cladding strain during a transient increases as the temperature rises. The strain remains below 1% until about 1900°F, even under the slowest, highest-pressure transient. Most of the deformation is shown (Figure 1) to occur in the very last stages of the transient.

As evident in Figure 1, the failure strains increased with decreasing failure temperatures, which in turn resulted from low transient rates and high internal pressures. Diametral strains do not exceed 17% even under the 10°F/sec, high-pressure transient conditions. Total hoop strains at failure reach about 60% during the 10°F/sec, high-pressure transient. For low stress levels, typical of beginning-of-life, unirradiated fuel cladding loadings (1300 psi hoop stress), the total hoop strains are only 0.5% and thus would not interfere with coolant flow.

The hoop stress in the cladding wall is plotted in Figure 2 against the failure temperature of unirradiated specimens tested to failure. This figure clearly illustrates the effect of hoop stress and transient heating rate on the failure temperature of this material. Failure will occur at a higher temperature during a 200°F/sec thermal transient than during a 10°F/sec transient under the same stress condition, because there is less time for annealing and time-dependent (creep) deformation during the higher heating rate.

Irradiated Cladding

The results from transient tests performed on irradiated cladding are summarized in Table II. The irradiation conditions and pertinent transient parameters are also summarized in this table. Figure 3 illustrates these data in terms of strain as a function of temperature attained during the transient. All of the irradiated cladding specimens were tested to failure. Both the diametral strain and total hoop strain at the failure site decrease with increasing failure temperature just as in the case of the unirradiated properties. However, the strains at failure were significantly reduced due to irradiation. The diametral strain away from the failure site is reduced to about 1.5% at a failure temperature of 2050°F and to about 1% between 2200 and 2400°F. The total hoop strain at the failure site is reduced to about 2% at 2050°F and to about 1.2% between 2200 and 2400°F.

TABLE I

UNIRRADIATED 20% C.W. TYPE 316 STAINLESS STEELCLADDING THERMAL TRANSIENT RESULTS

Spec. Ident.	Hoop Stress psi	Initial Test Temp., °F	Transient Heat Rate, °F/sec	Diametral Strain, %	Total Hoop Strain, %	Termination or Failure Temp., °F
4	3240	1110	10	2.5	NA ⁽¹⁾	2200
5	5400	1110	10	13.0	55	2110
6	5400	1110	200	9.0	28	2230
7	3240	1110	200	4.6	8.7	2350
8	3240	1110	200	3.4	NA	2260
9	3600	1350	10	3.3	NA	2250
10	3600	1350	200	2.3	NA	2270
11	6480	1350	10	5.5	61	2120
12	6480	1350	200	19.9	38	2260
13	3240	1110	200	1.3	NA	2050
14	3240	1110	10	1.5	NA	2050
15	5400	1110	10	6.6	NA	2050
16	5400	1110	200	2.1	NA	2050
17	3240	1110	10	7.0	NA	2250
18	3600	1350	10	1.0	NA	2060
19	3600	1350	200	0.8	NA	2030
20	6480	1350	10	11.0	NA	2060
21	6480	1350	200	3.5	NA	2030
23	6480	1350	10	1.2	NA	1900
29	1300	1350	10	0.3	0.7	2350
30	3240	1350	10	2.4	21.6	2300
33	1300	1350	200	0.2	0.3	2420

(1) NA = Not available because test terminated prior to failure. The total hoop strain and diametral strain are the same.

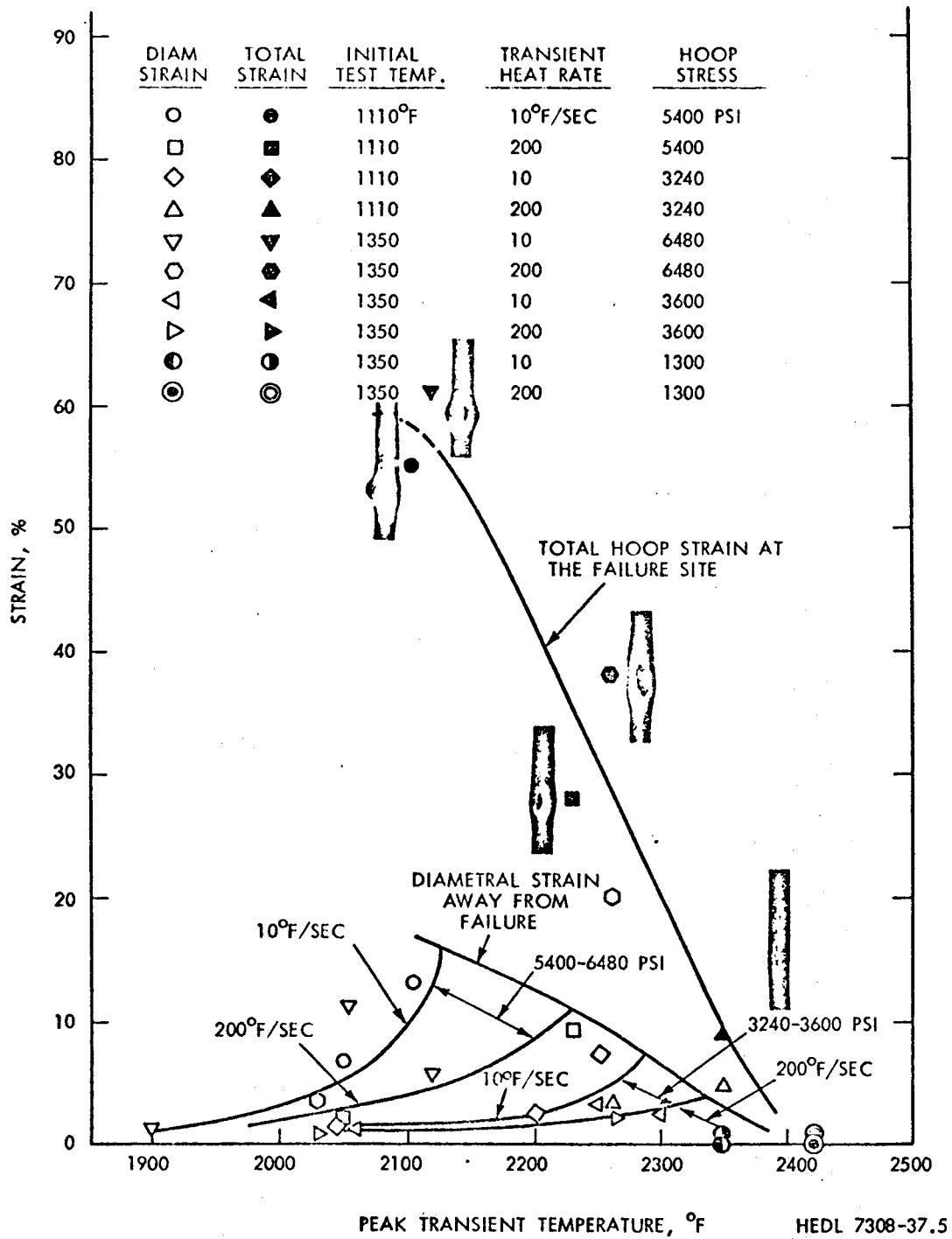


FIGURE 1. Strain of Unrradiated 20% C. W. Type 316 Stainless Steel Cladding During High Temperature Transients.

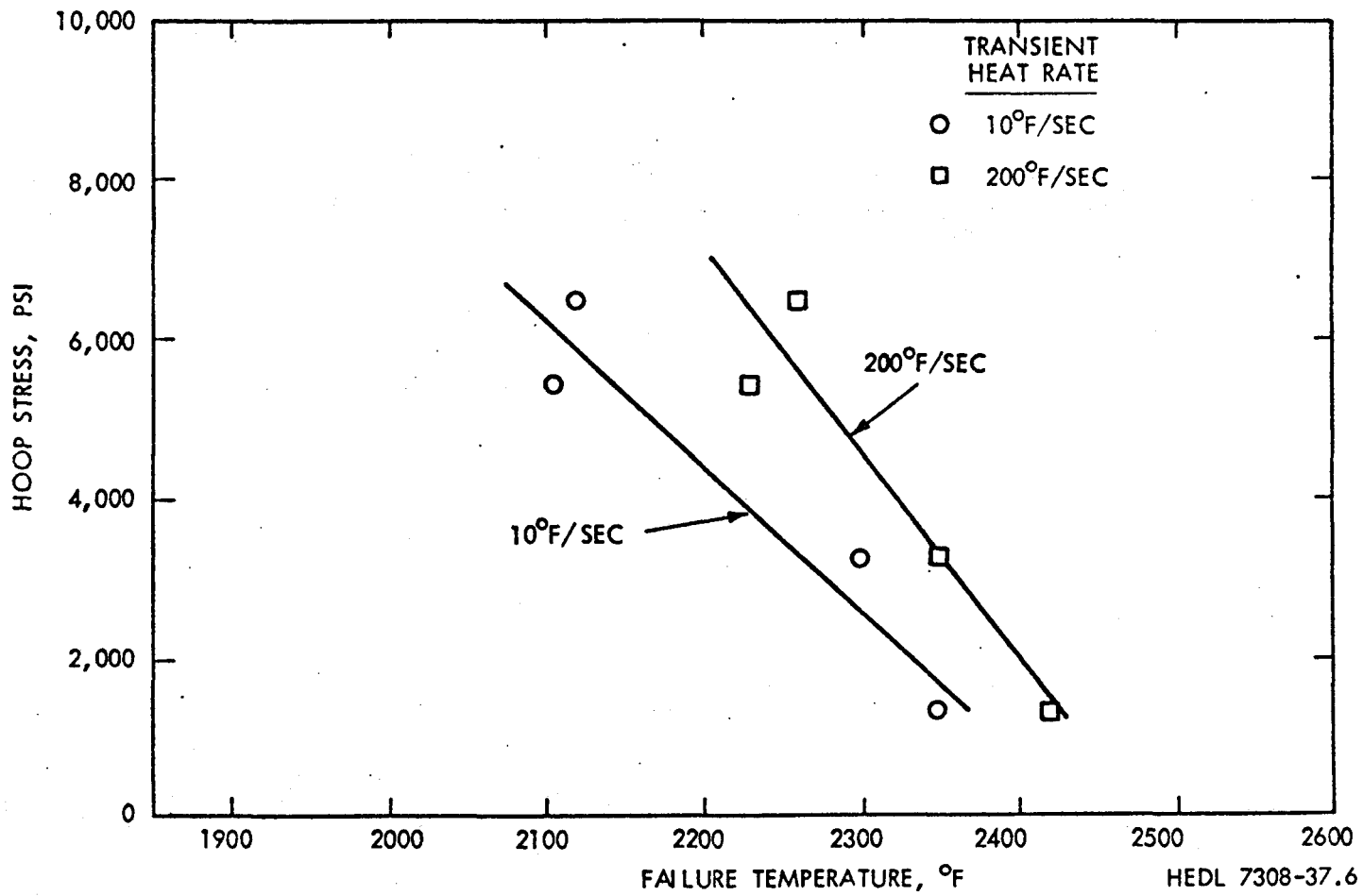


FIGURE 2. Effect of Hoop Stress on the Failure Temperature of Unirradiated 20% C.W. Type 316 Stainless Steel Cladding During High Temperature Transients.

TABLE II

EBR-II IRRADIATED 20% C.W. TYPE 316 STAINLESS STEELCLADDING THERMAL TRANSIENT RESULTS

Spec. Ident.	<u>IRRADIATION CONDITIONS</u>		Hoop Stress, psi	Initial Test Temp., °F	Transient Heat Rate, °F/sec	Diametral Strain, %	Total Hoop Strain, %	Failure Temp.
	Temp., °F	Fluence, n/cm ² (E > 0.1 MeV)						
E12	1410	9.0 x 10 ²¹	6480	1350	10	1.9	2.3	2060
E14	1410	9.0 x 10 ²¹	6480	1350	200	0.4	---	2210
E11	1420	9.0 x 10 ²¹	3600	1350	10	0.8	1.3	2200
E13	1420	9.0 x 10 ²¹	3600	1350	200	1.0	0.9	2280
E16	1410	9.0 x 10 ²¹	1300	1350	10	1.0	1.3	2380
C52	1050	7.4 x 10 ²¹	5400	1110	10	1.4	2.4	2030
C46	1050	7.4 x 10 ²¹	5400	1110	200	1.2	1.8	2170
C51	1060	7.4 x 10 ²¹	3240	1110	10	1.2	1.1	2190
C47	1050	7.4 x 10 ²¹	3240	1110	200	0.7	1.3	2210

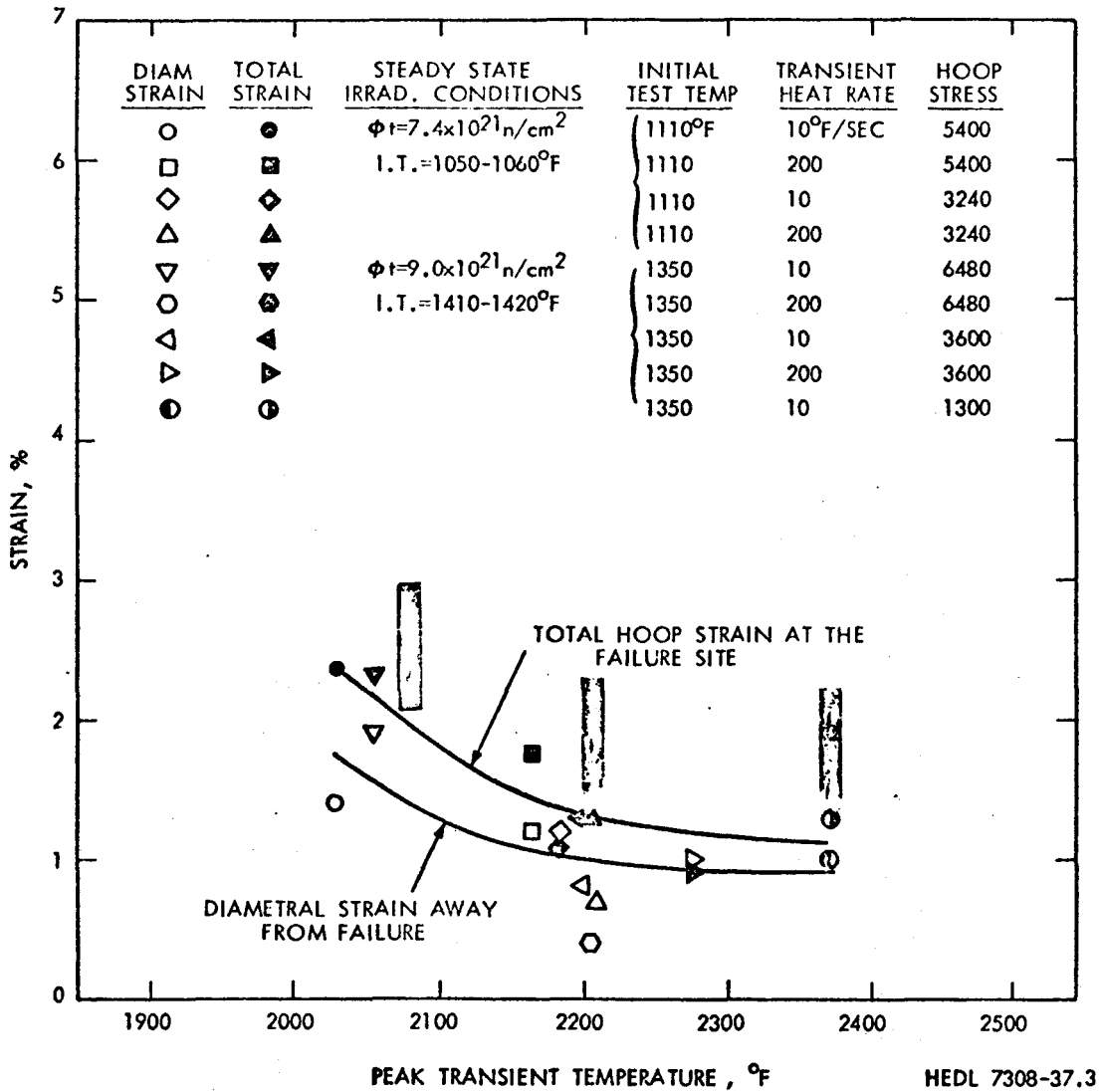


FIGURE 3. Failure Strain of Irradiated 20% C.W. Type 316 Stainless Steel Cladding During High Temperature Transients.

Since interrupted tests were not performed on irradiated specimens, the strain-temperature behavior has not been shown on this figure. However, it may be noted that the irradiated specimens in general exhibited lower failure strains at any particular temperature during the transient than the unirradiated specimens under the same loading and heating rate conditions.

The effect of fast reactor irradiation on the strain at failure of this material is more clearly illustrated in Figure 4. This plot shows that irradiation under the conditions previously outlined ($7.4-9.0 \times 10^{22}$ n/cm², 1050-1420°F) results in a thirty (30) fold decrease in total hoop strain at a failure temperature of 2100°F. The diametral strain away from the failure site is reduced by a factor of thirteen (13) at 2100°F. The reductions in strains due to irradiation decrease with higher failure temperatures.

The hoop stresses applied to the irradiated specimens are plotted against failure temperature in Figure 5. The effects of hoop stress, transient heating rate and irradiation temperature on the failure temperature are clearly illustrated in this figure. As in the case of the unirradiated material, the stress level required to cause failure decreases with increasing failure temperature. The higher heating rate also results in a higher failure temperature under the same hoop stress levels. The unirradiated material data did not indicate a strong effect of initial test temperature on the failure temperature. However, after irradiation a distinct trend exists in the failure temperature data with regard to the initial test temperature and irradiation temperature. The higher irradiation temperature (1410-1420°F) resulted in higher failure temperatures at any particular stress level. This higher strength behavior existed at both the 10°F/sec and 200°F/sec heating rates.

The effect of fast neutron irradiation on the failure temperature of 20% cold worked Type 316 stainless steel is also illustrated in Figure 5. The unirradiated trend lines are shown as dashed in this figure with the irradiated properties as solid lines. The exhibited decreases in failure temperature range from 25 to 100°F. It is clear that the cladding irradiated at the lower temperature showed the greatest decrease in failure temperature.

The irradiated specimens exhibited both lower failure strains and lower failure temperatures than the unirradiated cladding as illustrated in Figures 4 and 5. These effects are due primarily to the generation of helium during irradiation by (n,α) reactions at or very near to the grain boundaries. The helium assists the grain boundary separation during deformation. (10,11)

Figure 6 presents photographs of the irradiated specimens which are arranged for convenient comparison of irradiation, hoop stress, and thermal transient rate effects. This figure allows a pictorial evaluation of these effects and of the failure character. Under high pressures (5400-6480 psi hoop) the extensive ductility of unirradiated cladding is readily apparent. Even though the fracture site has opened wide in some of the irradiated specimens, the actual total hoop strain values are small.

The openings of the failure sites are dependent upon the quantity and pressure of gas, as well as material behavior. Therefore, the opening exhibited in these tests cannot be universally applied to other specific cases. Probably the openings are larger than would initially occur at the top of the fuel column in a fuel pin, because of the gas flow restriction provided by the fuel.

SUMMARY

The stress-strain and failure behavior of fast reactor 20% cold worked Type 316 stainless steel fuel cladding has been experimentally defined, under

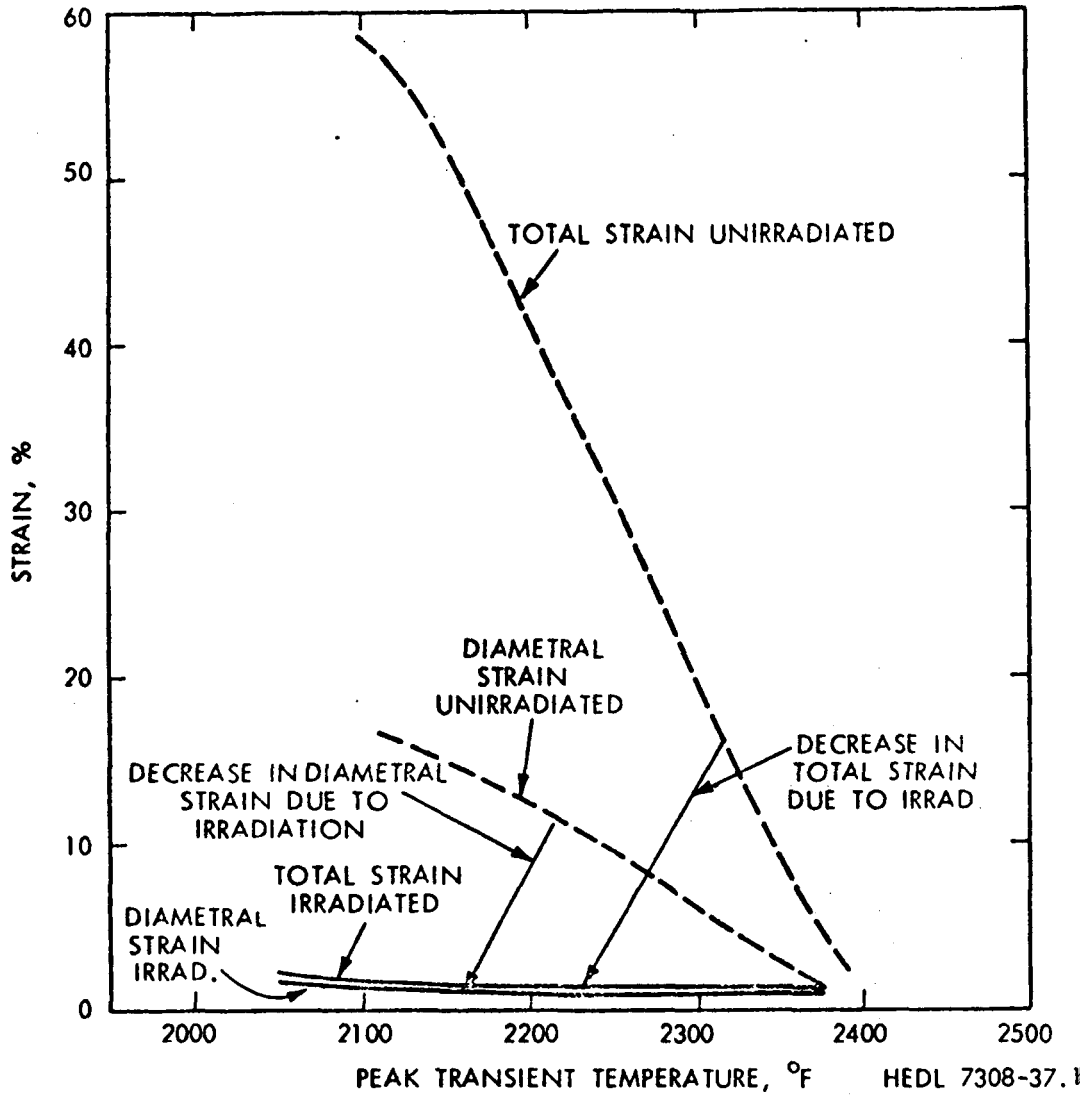


FIGURE 4. Effect of Irradiation on the Failure Strain of 20% C.W. Type 316 Stainless Steel Cladding During High Temperature Transients.

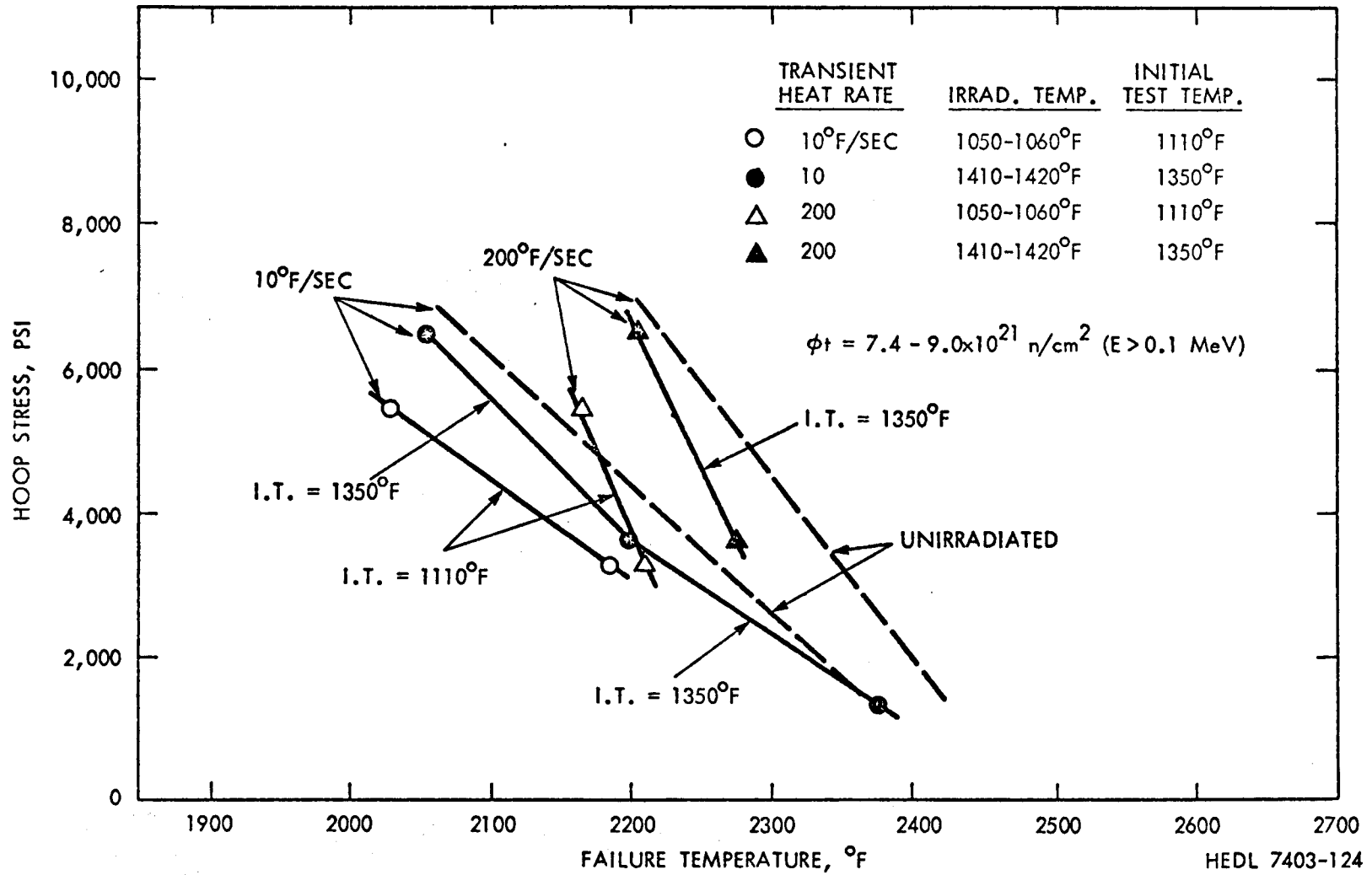


FIGURE 5. Effect of Hoop Stress on the Failure Temperature of Irradiated 20% C.W. Type 316 Stainless Steel Cladding During High Temperature Transients.

INITIAL TEMPERATURE
1110°F

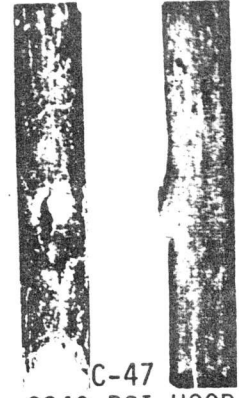
TEMPERATURE TRANSIENT RATE
200°F/SEC



6
5400 PSI HOOP
UNIRRADIATED
2230°F PEAK
 $\epsilon_t = 28\%$



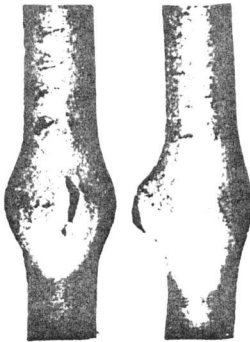
C-46
5400 PSI HOOP
 7.4×10^{21} @1050°F
2170°F PEAK
 $\epsilon_t = 1.8\%$



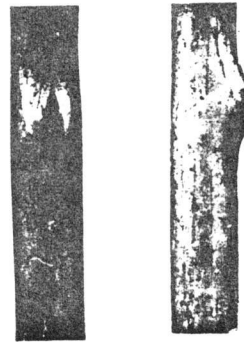
C-47
3240 PSI HOOP
 7.4×10^{21} @1050°F
2210°F PEAK
 $\epsilon_t = 1.3\%$

INITIAL TEMPERATURE
1350°F

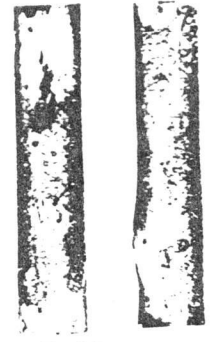
TEMPERATURE TRANSIENT RATE
10°F/SEC



11
6480 PSI HOOP
UNIRRADIATED
2120°F PEAK
 $\epsilon_t = 61\%$



E-12
6480 PSI HOOP
 9×10^{21} @1410°F
2060°F PEAK
 $\epsilon_t = 2.3\%$



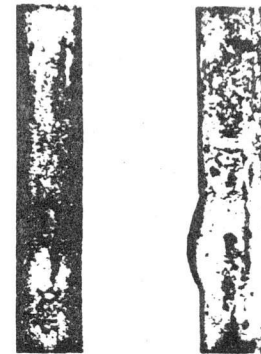
E-11
3600 PSI HOOP
 9×10^{21} @1420°F
2200°F PEAK
 $\epsilon_t = 1.3\%$

INITIAL TEMPERATURE
1350°F

TEMPERATURE TRANSIENT RATE
10°F/SEC



29
1300 PSI
UNIRRADIATED
2350°F PEAK
 $\epsilon_t = 0.7\%$



E-16
1300 PSI
 9×10^{21} @1410°F
2375°F PEAK
 $\epsilon_t = 1.3\%$

FIGURE 6. Irradiated and Unirradiated 20% C.W. 316 SS Fuel Cladding Failed During Simulated Loss-Of-Flow Temperature Transients.

the loading and temperature transient conditions of interest to the analysis of hypothetical LOF transients. Both unirradiated and low-fluence ($7.4-9.0 \times 10^{21}$ n/cm², $E_n > 0.1$ MeV) cladding specimens were subjected to hoop stresses of 1300 through 6480 psi (approximating beginning, through high-burnup fission gas loadings) with temperature transients of 10 and 200°F/sec. The principal results and conclusions are:

- 1) At the lowest hoop stress of 1300 psi, which is characteristic of beginning-of-life unirradiated cladding, the beginning of deformation and ultimate failure were essentially simultaneous at about 2400°F. The total hoop strain is only about 0.5%, so that cladding deformations could not interfere with coolant flow.
- 2) For the highest stress (6480 psi hoop), deformation began at 1900-2000°F in the unirradiated cladding, and failure occurred at 2100-2200°F. For this situation the ductility was very high with diametral strains of 12-17% away from the failure site and total hoop strains of 30-60% at the failure site. However, this situation is not typical of the low pressures expected at beginning-of-life.
- 3) For lower stresses the unirradiated behavior was similar, except that deformation and failure occurred at higher temperatures, and the failure strain values were reduced at the failure site and away from it.
- 4) The slower heating rate, 10°F/sec, produced deformation and failure at lower temperatures.
- 5) The low-fluence irradiation greatly reduced the failure ductilities. Even at the highest stresses, indicative of end-of-life loading where the irradiated ductility was the greatest, the total hoop strain was only 2.4%, so that cladding ballooning could not interfere with coolant flow.
- 6) The failure temperature of the irradiated cladding was reduced at equivalent hoop stress levels from the unirradiated cladding failure temperatures.

REFERENCES

1. A. D. Emery, D. B. Scott, J. R. Stewart, "Effects of Heating Rate and Pressure on Expansion of Zircaloy Tubing During Sudden Heating Conditions," Nuclear Technology, Vol. 11, No. 4, August 1971, p.474.
2. D. O. Hobson, M. F. Osborn, G. W. Parker, "Comparison of Rupture Data from Irradiated Fuel Rods and Unirradiated Cladding," Nuclear Technology, Vol. 11, No. 4, August 1971, p. 479.
3. R. D. Waddell, Jr., "Measurements of Light-Water Reactor Channel Reduction Arising from Cladding Deformation During a Loss-Of-Coolant Accident," Nuclear Technology, Vol. 11, No. 4, August 1971, p. 491.
4. R. A. Lorenz, D. O. Hobson, G. W. Parker, "Fuel Rod Failure Under Loss-Of-Coolant Conditions in TREAT," Nuclear Technology, Vol. 11, No. 4, August 1971, p. 502.
5. M. M. Paxton, "Mechanical Properties of Prototypic FTR Cladding--20% C.W. 316 Stainless Steel Tubing," HEDL-TME 71-59, April 1971.
6. D. Fahr, "Precipitate-Free Ultra-Fine Grains, A New Approach to Heat Treatment," ORNL-TM-3550, December 1971.
7. M. M. Paxton and J. J. Holmes, "Recovery and Recrystallization of Prototypic FTR Fuel Cladding--20% C.W. 316 Stainless Steel Tubing," HEDL-TME 71-126, September 1971.
8. H. K. Fauske, "Evaluation of Dryout and Flow Instability in the Wake Downstream of a Blockage in an LMFBR Subassembly," Trans. ANS, Vol. 15, No. 1, June 18-22, 1972.
9. W. N. McElroy, et. al., Nucl. Sci. Engr., Vol. 36, p.15, 1969.
10. R. S. Barnes, Nature, Vol. 206, p. 1307, 1965.
11. D. Kramer, H. R. Brager, C. G. Rhodes, and A. G. Pard, "Helium Embrittlement in Type 304 Stainless Steel," J. Nucl. Matls., Vol. 25, pp. 121-130, 1968.